

A New Medical Image Registration^{*}

Meisen Pan^{*}, Fen Zhang, Jianjun Jiang

*College of Computer Science and Technology, Hunan University of Arts and Science
Changde 415000, China*

Abstract

This proposed method calculates the centroids of two registering images by applying the moments for acquiring the original displacement parameters, and then uses modified K-means clustering to classify the image coordinates. Before clustering, the medical image coordinates is centralized, the two-row coordinate matrix is created to construct the 2-D sample set to be partitioned into two classes, the slope of a straight line fitted to the two classes is computed, and the rotation angle is computed by solving the arc tangent of the slope. The edges are detected by the edge convolution kernel and the binary images covering the characteristic points are extracted. Experimental results from aligning experiments reveal that, this approach has lower computation costs and a higher registration precision.

Keywords: Centroids; Image Registration; K-means Clustering; Iterative Closest Points

1 Introduction

Medical image registration signifies that the space geometry transform is applied to register several images created by various imaging devices, and makes the pixels (voxels) expressing the identical construction be the same spatial position [1,2]. After years of development and evolution, the methods for registering medical images have achieved rapid advance, and global experts and scholars have proposed many practical and effective technologies. Among these methods, characteristic-based image approaches have been extensively applied for aligning medical images [3]. For the characteristic-based alignment method, in essence, it extracts the conjunct, distinct and significant characteristics between the aligning the objects to explore the transform values. It is effective and easy to implement, while its alignment precision seriously counts on whether it can exactly extract the critical characteristic points [4–7]. In consideration of the complication of various images, it is really an intractable issue to solve the fully-automated and accurate abstraction and refinement of the useful characteristic points from medical images. So its poor adaptability and robustness need to be further boosted.

^{*}Project supported by the Key Scientific Research Fund of Hunan Provincial Education Department, China (No. 13A064), the Construct Program of the Key Discipline in Hunan University of Arts and Science, and the Doctor Scientific Research Startup Project Foundation of Hunan University of Arts and Science.

^{*}Corresponding author.

Email address: pmsjjj@126.com (Meisen Pan).

In 1980's, the researchers made deep and systematic study about the registration of set of points. In particular, Arun et al. [8] introduced an approach to alignment between point sets using unit quaternion to represent rotation in 1987. A lot of aligning experiments have shown that the registration technology is an appreciated way to confront the thorny issues of alignment. In 1992, Besl et al. [9] pioneered the Iterative Closest Point (ICP) algorithm, to handle the problem of registration of point sets. ICP, as a characteristic-based registration method, is a very famous method and widely put into use in the registration of set of points. It can align the set of points without the requirement for segmentation or other preprocessing of the images. Therefore, it is more propitious for registering set of points [2]. So it is widely used in various alignment fields. However, it exists some problems that need to be resolved in the implement process. First, it must repetitive and iteratively explore the closest points, and as a result the computation costs are extremely expensive. Second, whether ICP can exactly derive the optimal registration parameters seriously dependent on the selection of the original rotation and displacement parameters. If the original values are not fitted to respond to ICP, then the registering operation has to take more time to explore the optima and even results in failure. In addition, it is troublesome to select the pivotal characteristic points delineating the object outline automatically when aligning images. Furthermore, it can effortlessly fall in the trap of the local optima.

In order to tackle the problems mentioned above, on the foundation of an in-depth study about the K-means Clustering (KMC) and ICP, we present medical image registration using Modified K-means Clustering (RMKMC).

2 Medical Image Registration Using Modified K-Means Clustering

2.1 ICP

Assume that sets $\mathbf{S}, \mathbf{F} \in R^K$, $\mathbf{S} = \{\mathbf{s}_i, i = 1, 2, \dots, N\}$ with $\mathbf{s}_i = [s_{i1} \dots s_{iK}]^T$ and $\mathbf{F} = \{\mathbf{f}_j, j = 1, 2, \dots, M\}$ with $\mathbf{f}_j = [f_{j1} \dots f_{jK}]^T$ present the reference and floating sets respectively, and $\mathbf{Z} = \{\mathbf{z}_i, i = 1, 2, \dots, M\}$ with $\mathbf{z}_i = [z_{i1} \dots z_{iK}]^T$ and $\mathbf{z}_i \in \mathbf{S}$ expresses the closest point set. In addition, \mathbf{R}_0 and \mathbf{T}_0 denote $K \times K$ rotation and $K \times 1$ matrices respectively. ICP introduced by Besl and McKay is aimed at exploring a rigid transformation $(\mathbf{R}_0, \mathbf{T}_0)$ to make the mean square sum representing the Euclidean distances between the set \mathbf{F} mapped by $(\mathbf{R}_0, \mathbf{T}_0)$ and its closest point set \mathbf{Z} in \mathbf{S} be minimized, i.e., the objective function

$$J(\mathbf{R}_0, \mathbf{T}_0) = \text{Min} \left\{ \frac{1}{M} \sum_{i=1}^M \|\mathbf{z}_i - (\mathbf{R}_0 \cdot \mathbf{f}_i + \mathbf{T}_0)\| \right\} \quad (1)$$

here \mathbf{R}_0 is computed by the unit quaternion [9], and then \mathbf{T}_0 is obtained by

$$\mathbf{T}_0 = \bar{\mathbf{z}} - \mathbf{R}_0 \cdot \bar{\mathbf{f}} \quad \left(\bar{\mathbf{z}} = \frac{1}{M} \sum_{i=1}^M \mathbf{z}_i, \bar{\mathbf{f}} = \frac{1}{M} \sum_{i=1}^M \mathbf{f}_i \right) \quad (2)$$

In ICP, the original rotation matrix \mathbf{R}_0^0 and the translation matrix \mathbf{T}_0^0 are set by $\begin{bmatrix} 1 & 0 & 0 \\ 0 & 1 & 0 \\ 0 & 0 & 1 \end{bmatrix}$

and $[0 \ 0 \ 0]^T$ respectively. Further, \mathbf{f}_j^0 representing the component of the original set \mathbf{F}^0 is $\mathbf{f}_j^0 = \mathbf{R}_0^0 \cdot \mathbf{f}_j + \mathbf{T}_0^0 = \mathbf{f}_j (j = 1, 2, \dots, M)$, i.e., $\mathbf{F}^0 = \mathbf{F}$. In essence, ICP is the process that the iteration is repeated until $J(\mathbf{R}_0, \mathbf{T}_0)$ meets a given threshold which denotes the expected alignment precision or the iteration number exceeds a given parameter.

According to the description above, ICP has a heavily computational load, is greatly influenced by original rotation and translation matrices, and easily traps into the local optima.

2.2 Acquisition of the Centroids

Let $f(x, y)$ be a two-dimensional discrete image, the following equation defines its moment in order $(s + t)$ can be defined by [10]

$$M_{s,t} = \sum_{x=1}^M \sum_{y=1}^N x^s y^t f(x, y) \quad s, t = 0, 1, 2, \dots \quad (3)$$

where $(s + t)$ expresses the order and, M and N are the sampling point numbers in image space. And well we can define the zeroth as follows [10]

$$M_{0,0} = \sum_{x=1}^M \sum_{y=1}^N f(x, y) \quad (4)$$

Further, when $s = 1$ and $t = 0$, and, $s = 0$ and $t = 1$ [10],

$$\bar{x} = \frac{M_{1,0}}{M_{0,0}}, \quad \bar{y} = \frac{M_{0,1}}{M_{0,0}} \quad (5)$$

here we define (\bar{x}, \bar{y}) as the centroids of an object.

2.3 Calculation of the Rotation Angle Using MKMC

KMC proposed by MacQueen in 1967 divides the data into the preset classes by minimizing the error function. The principle of KMC is simple and is easy to deal with a lot of data. In addition, the number of classes and iterations or the convergence condition of KMC must be assigned in advance, and the initial cluster centers also have to be designated. Based on certain similarity metric, each sample is allocated into the nearest or the most similar clustering center to form a class set, then the average vector of each class set is viewed as the cluster center of the class set, therefore each sample is reallocated into the new cluster center. The above process is iterated until the convergence condition is fulfilled or the maximum number of iterations is achieved.

2.3.1 KMC

Let $\mathbf{S} = \{\mathbf{s}_1, \mathbf{s}_2, \dots, \mathbf{s}_n\}$, be a set containing n samples for $\mathbf{s}_i = [s_{i1}, s_{i2}, \dots, s_{il}]^T (i = 1, 2, \dots, n)$, $\mathbf{P} = \{\mathbf{p}_1, \mathbf{p}_2, \dots, \mathbf{p}_c\}$ expresses a cluster center set with the element number c , the element $\mathbf{p}_j = [p_{j1}, p_{j2}, \dots, p_{jk}]^T (j = 1, 2, \dots, c)$ represents the center of the j th class including r_j samples,

and \mathbf{s}_k^j denotes the k th sample in the j th class with $j = 1, 2, \dots, c$ and $k = 1, 2, \dots, r_j$. Therefore, the cluster center of each class is expressed

$$\mathbf{p}_j = \frac{1}{r_j} \sum_{k=1}^{r_j} \mathbf{s}_k^j \quad (\mathbf{s}_k^j \in \mathbf{S}) \quad (6)$$

Thus, the object function of clustering can be formulated as

$$J(\mathbf{S}, \mathbf{P}) = \sum_{j=1}^c \sum_{k=1}^{r_j} d(\mathbf{s}_k^j, \mathbf{p}_j) \quad (7)$$

where \mathbf{P} is the set of the cluster centers, and $d(\mathbf{s}_k^j, \mathbf{p}_j)$ is the distance between the sample \mathbf{s}_k^j and its corresponding cluster center \mathbf{p}_j . The purpose of KMC is to obtain \mathbf{P} in the case of minimizing the above object function $J(\mathbf{S}, \mathbf{P})$.

When performing KMC, in general, we select the Euclidean distances as the distance metric $d(\mathbf{s}_i, \mathbf{p}_j)$, i.e., $d(\mathbf{s}_i, \mathbf{p}_j) = \|\mathbf{s}_i - \mathbf{p}_j\|^2$. Furthermore, we have to mention that the clustering results from KMC are heavily dependent on the original cluster centers selected. Generally, if the original cluster centers selected are a serious departure from the global optimal partition, then KMC possibly gets into the local optimal solution. Also, the greater the number of classes is, the more obvious the issue is. Therefore, a larger number of iterations are possibly required to obtain the satisfactory results.

2.3.2 Selection of the Original Cluster Center Sets of MKC

According to the description of the algorithm, KMC, due to its strong sensitivity to the original cluster center set, possibly gets a dubious result. For two medial images in Fig. 1, for example, when a cluster center set is randomly chosen, we use KMC to handle each image by 10 operations respectively and obtain the relationship among the original cluster center set, the derived angle and the running time of MKC, illustrated in Fig. 2.

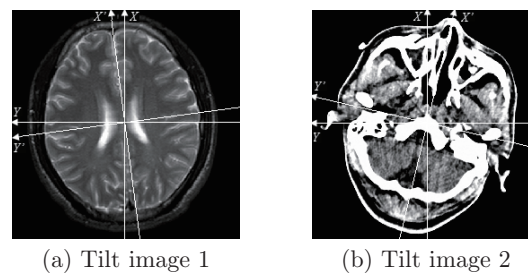


Fig. 1: Tilt medical images

In Fig. 2, the two tilt (rotation) angles obtained by MKC are swinging, varying in a certain range and existing several local pitfalls. As the result, the uncertain tilt (rotation) angles cause the corresponding indeterminate rotated images by the negative tilt (rotation) angles, which will negatively and harmfully influence the successive image processing; and at the same time the amplitude fluctuation of the running time is relatively greater. Therefore, it is very necessary to pick out a suitable original cluster center set.

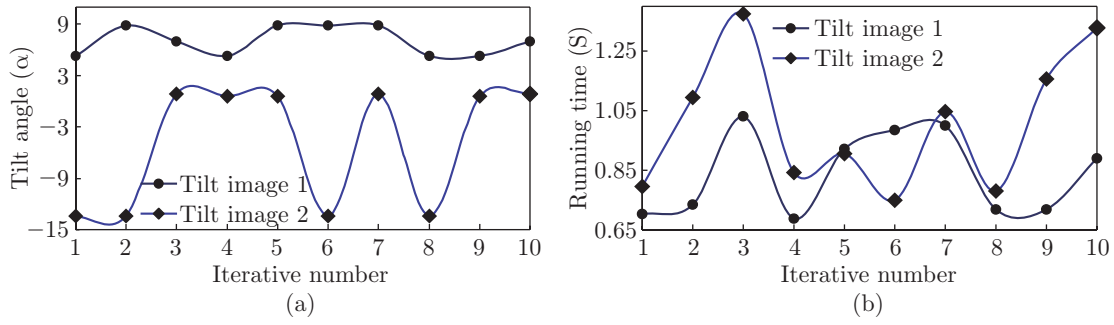


Fig. 2: The relationship among a random initial cluster center set, the derived angle, and the running time. (a) The derived angle in the case of the random selection of an initial cluster center set; (b) The running time in the case of the random selection of an initial cluster center set

In this paper, we will initialize the cluster center set according to the following method: First, for the number n of elements in the sample set \mathbf{S} , we compute $half = integer[n/2]$. Then, the sample set \mathbf{S} is divided into two class subsets: the first $half$ samples in \mathbf{S} constitute one class subset and the remainder forms another class one. Finally, the center vectors of the two class subsets are computed respectively, namely

$$\mathbf{p}_1 = \frac{1}{half} \sum_{i=1}^{half} \mathbf{s}_i, \quad \mathbf{p}_2 = \frac{1}{n - half} \sum_{i=half+1}^n \mathbf{s}_i \tag{8}$$

For the two images in Fig. 1, the original cluster center sets are first derived based on Eq. (8) and then the relationships among the original cluster center sets, the derived angle and the running time of KMC are acquired respectively, shown in Figs. 3 (a) and 3 (b). Now we can observe, the derived angles from the two tilt (rotation) images are jarless and accurate, which is conducive to get the registration original values. Moreover, the amplitude fluctuation of the running time is relatively less.

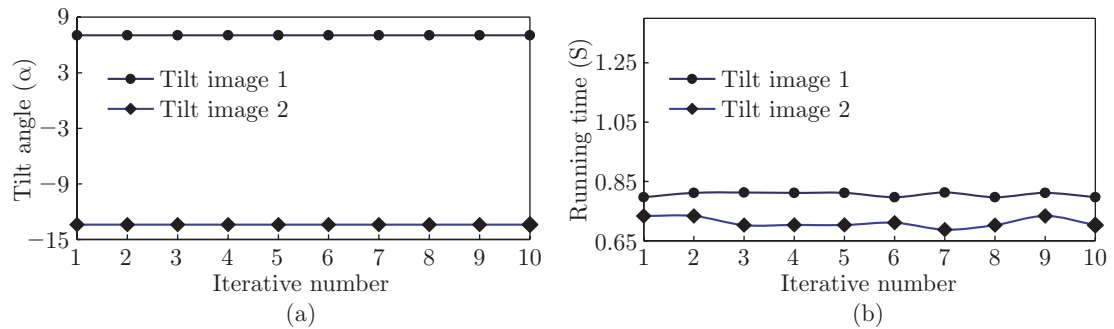


Fig. 3: The relationship among the initial cluster center set created by Eq. (8), the derived tilt angle, and the running time. (a) The derived angle in the case of the initial cluster center set generated by Eq. (8); (b) The running time in the case of the initial cluster center set created by Eq. (8)

2.3.3 Calculation of the Rotation Angle

Taken together, we elaborate Acquisition of Rotation Angle Using Modified K-Means Clustering (MKMC) as argued below.

Step 1. The BSGO is applied to acquire the edges of the original image \mathbf{F} and create the binary edge image \mathbf{Bin} .

Step 2. The bounding box of \mathbf{Bin} including top, bottom, left, and right boundaries, is probed.

Step 3. On the basis of the bounding box of \mathbf{Bin} , the subimage \mathbf{F}_{Sub} is unearthed from the image \mathbf{F} .

Step 4. Based on Eqs. (3) and (4), the moments $M_{0,0}$, $M_{1,0}$ and $M_{0,1}$ of \mathbf{F}_{Sub} are counted respectively.

Step 5. According to Eq. (5), the centroid coordinates (\bar{x}, \bar{y}) of \mathbf{F}_{Sub} are derived.

Step 6. The image matrix \mathbf{P}_r is built, namely, the coordinate origin is moved to the centroids of \mathbf{F}_{Sub} , which means that the coordinates of \mathbf{F}_{Sub} are centralized. \mathbf{P}_r denotes the two-row matrix of the coordinates (x, y) of pixel points in the sub-image \mathbf{F}_{Sub} , where the number of elements (namely the number of columns) is $(H \times W)$, that is, $\mathbf{P}_r \in R^{2 \times (H \times W)}$.

$$\begin{cases} \mathbf{P}_r((t-1) \times W + q, 1) = (t - \bar{x}) \times \mathbf{F}_{Sub}(t, q) \\ \mathbf{P}_r((t-1) \times W + q, 2) = (q - \bar{y}) \times \mathbf{F}_{Sub}(t, q) \end{cases} \quad (9)$$

here $t = 1, 2, \dots, H$; $q = 1, 2, \dots, W$.

Step 7. According to \mathbf{P}_r with size being $n = H \times W$, we compute $half = integer[n/2]$, and then \mathbf{P}_r is divided into two class subsets: the first $half$ samples in it constitute one class subset and the remainder forms another class subset. Finally, the center vectors of the two class subsets are computed respectively according to Eq. (8) to get the original cluster center sets of KMC.

Step 8. \mathbf{P}_r is grouped into two classes $\mathbf{p}_j = [p_{j,1}, p_{j,2}]^T$ ($j = 1, 2$) by KMC.

Step 9. A straight line is used to be fitted through the two classes and the corresponding slope k is obtained

$$k = \frac{p_{2,2} - p_{1,2}}{p_{2,1} - p_{1,1}} \quad (10)$$

Step 10. The tilt (rotation) angle α is computed according to k

$$\alpha = \arctan\left(\frac{1}{k}\right) * \frac{180}{\pi} \quad (11)$$

2.4 RMKMC

The original rotation matrix \mathbf{R}_0^0 and translation matrix \mathbf{T}_0^0 of ICP are computed by applying MKMC and the centroid coordinates respectively, and the reference and floating point sets are extracted by BSGO. As mentioned previously, medical image registration using Modified k-means clustering is described below.

Step 1. Compute the centroids (\bar{x}_S, \bar{y}_S) and (\bar{x}_F, \bar{y}_F) , and the rotation parameters α_S and α_F of the images \mathbf{S} and \mathbf{F} respectively based on the moments and MKMC of the images.

Step 2. Derive the original values for registration from the following expressions

$$\Delta x = (\bar{x}_F - \bar{x}_S), \Delta y = (\bar{y}_F - \bar{y}_S), \Delta \alpha = (\bar{\alpha}_F - \bar{\alpha}_S)$$

Step 3. Use Δx , Δy and $\Delta\alpha$ as the original rotation and translation values for performing ICP. That is,

$$\mathbf{R}_0^0 = \begin{bmatrix} \cos(\Delta\alpha) & -\sin(\Delta\alpha) \\ \sin(\Delta\alpha) & \cos(\Delta\alpha) \end{bmatrix}, \quad \mathbf{T}_0^0 = [\Delta x \ \Delta y]^T$$

Step 4. Impose BSGO on the images \mathbf{S} and \mathbf{F} respectively, and generate the binary images \mathbf{Bin}_S and \mathbf{Bin}_F with gray value being 0 or 1.

Step 5. Extract two point sets of coordinates on behalf of the whole pixels whose grayscale values are 1 in \mathbf{Bin}_S and \mathbf{Bin}_F respectively for the reference and floating point sets in ICP.

Step 6. Perform ICP and derive the final rotation and translation matrices \mathbf{R}_0 and \mathbf{T}_0 .

3 Experiments and Results

We derive the test images from the image library of the human brain founded by RREP, attached to Vanderbilt University, USA. RMKMC is performed in MATLAB 7.1 on a personal computer with an Intel Dual-Core E5500 2.80 GHz and 2 GB RAM, running Windows XP. For the sake of verifying RMKMC with a rapid performance, good alignment accuracy and a strong reliability, we carry out RMKMC and compare the results from ICP. In the aligned images shown below, the red and green marks express the consequences from extraction of the experimental images by the edge detection operator Canny respectively, while the yellow ones label the corresponding part of the aligned images. In order to assess the registration accuracy, we use error ρ in [2].

In the experiment, we use No.5 CT, MR_PD_rectified No.6 and PET No.3 brain images of the training_007 to be used for the experimental objects with gray level being 256, and group them into the subsequent four groups. In the first group, we choose CT1 for the reference image and, MR1 for the floating image, with sizes being 256×256 , displayed in Fig. 4. In the second group, we select MR2 for the reference image and, CT2 for the floating one, with size being 256×256 , illustrated in Fig. 5. In the third group, we pick CT3 for the reference image and, PET1 for the floating one, with sizes being 128×128 , listed in Fig. 6. In the final group, we extract MR3



(a) CT1 reference image (b) MR1 floating image

Fig. 4: The first group



(a) MR2 reference image (b) CT2 floating image

Fig. 5: The second group



(a) CT3 reference image (b) PET1 floating image

Fig. 6: The third group



(a) MR3 reference image (b) PET2 floating image

Fig. 7: The fourth group

for the reference image and, PET2 for the floating one, with sizes being 128×128 , plotted in Fig. 7. Moreover, we demonstrate the comparatively precious transform values in Table 1, which are taken as Δi_s in Eq. (7) in [2].

Table 1: Transform values of multi-modality floating images

Floating images	Parameters		
	$\Delta x_s/Pixel$	$\Delta y_s/Pixel$	$\Delta \alpha_s/^\circ$
The first group	19.127	15.664	-12.652
The second group	23.197	-14.798	18.6136
The third group	18.0450	14.574	-14.368
The fourth group	-14.422	-10.858	9.787

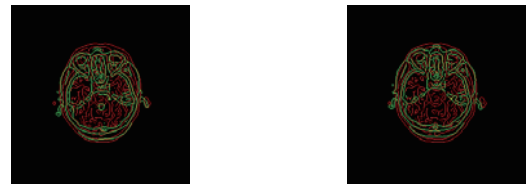
Just as before, ICP is first employed to align the images and then RMKMC to do the same. The experiment consequences are illustrated in Figs. 8-11 and Table 2.



(a) ICP

(b) RMKMC

Fig. 8: Result figures of the first group



(a) ICP

(b) RMKMC

Fig. 9: Result figures of the second group



(a) ICP

(b) RMKMC

Fig. 10: Result figures of the third group



(a) ICP

(b) RMKMC

Fig. 11: Result figures of the fourth group

According to Table 2, the aligning speed of RMKMC is relatively faster than that of ICP, particularly for the images with large size. From Figs. 8-11, ICP cannot match most of the experimental images except for the second group of images with a relatively lower total error. As for RMKMC, it is can succeed in aligning the whole experimental objects, which is consistent with the errors in Table 2. And yet, in the one case aligned by RMKMC, namely the alignment of CT3 and PET1, the accuracy is slightly inferior to those of aligning the other groups of images. As shown previously, the application of obtaining original rotation and displacement values from the multi-modality medical images is an appropriate approach. Therefore, on the whole, RMKMC can be applied for aligning the multi-modality medical images.

4 Conclusions

To deal with the congenital deficiencies of aligning the images using ICP, by applying MKMC and the centroids for obtaining the original parameters, and BGSO for selecting the characteristic

Table 2: Performance of aligning the images Figs. 9-11 applying ICP and RMKMC

Images	Methods	Parameters				Errors			
		$\Delta x/Pixel$	$\Delta y/Pixel$	$\Delta\alpha/^\circ$	$Time/S$	ρ_x	ρ_y	ρ_α	ρ
The first group	ICP	32.427	35.240	-7.2360	23.25	69.535	124.975	42.808	237.318
	RMKMC	17.591	15.797	-12.923	8.953	8.031	0.849	2.142	11.022
The second group	ICP	25.235	-15.865	20.337	24.985	8.786	7.210	9.259	25.255
	RMKMC	21.548	-15.072	17.686	10.390	7.109	1.852	4.984	13.945
The third group	ICP	10.268	19.536	-3.528	2.235	43.098	34.047	75.445	152.590
	RMKMC	18.908	13.516	-13.532	2.204	4.783	7.260	5.819	17.862
The fourth group	ICP	-14.379	-10.734	3.435	0.671	0.298	1.142	64.902	66.342
	RMKMC	-14.563	-11.053	9.070	0.588	0.978	1.796	7.326	10.100

points, RMKMC is presented. The experiments reveal that, RMKMC is easy to implement, has lower computation costs, higher registration precision, and a remarkable ability that avoids being caught in the local optima. RMKMC has a better performance in registering medical images.

References

- [1] M. Nejati, H. Pourghassem, Multiresolution image registration in digital X-ray angiography with intensity variation modeling [J], *Journal of Medical Systems*, 38(1), 2014, 10-18
- [2] M. S. Pan, J. J. Jiang, F. Zhang, X. Fang, Qiusheng Rong, Performance comparison of optimization methods for medical image registration [J], *Journal of Fiber Bioengineering and Informatics*, 7(4), 2014, 507-516
- [3] J. B. A. Maintz, M. A. Viergever, A survey of medical image registration [J], *Medical Image Analysis*, 2(1), 1998, 1-36
- [4] P. Hyunjin, H. Peyton, K. Kristy, Adaptive registration using local information measures [J], *Medical Image Analysis*, 8(4), 2004, 465-473
- [5] A. Can, C. Stewar, A feature-based, robust, hierarchical algorithm for registration palm of images of the curved human retina [J], *IEEE Transactions on Pattern Analysis and Machine Intelligence*, 24(3), 2002, 347-363
- [6] Y. Liu, H. D. Cheng, J. H. Huang, An effective non-rigid registration approach for ultrasound image based on “Demons” algorithm [J], *Journal of Digital Imaging*, 26(3), 2013, 521-529
- [7] W. Liu, E. Ribeiro, Incremental variations of image moments for nonlinear image registration [J], *Signal, Image and Video Processing*, 8(3), 2014, 423-432
- [8] K. S. Arun, T. S. Huang, S. D. Blostein, Least-squares fitting of two 3-D point sets [J], *IEEE Transactions on Pattern Analysis and Machine Intelligence*, 9(5), 1987, 698-700
- [9] P. J. Besl, N. D. McKay, A method for registration of 3-D shapes [J], *IEEE Transactions on Pattern Analysis and Machine Intelligence*, 14(2), 1992, 239-256
- [10] M. K. Hu, Visual pattern recognition by moment invariants [J], *IRE Transactions on Information Theory*, 8(2), 1962, 179-187